Diverse Applications of Einstein's Equations of General Relativity

R. Wayte.

29 Audley Way, Ascot, Berkshire, SL5 8EE, England, UK.

Email: rwayte@googlemail.com

Submitted to vixra.org 21 November 2019

Abstract: This paper comprises extracts from previous articles showing how Einstein's general relativity equations can describe different forces by substituting the associated constants. The articles depended upon a new solution of Einstein's equations which is compatible with electromagnetic theory.

> A theory is the more impressive the greater the simplicity of its premises is, the more different kinds of things it relates, and the more extended its area of applicability.....I do not see any reason to assume that the heuristic significance of the principle of general relativity is restricted to gravitation ..... a deeper knowledge of the foundations of physics seem doomed to me unless the basic concepts are in accordance with general relativity from the beginning...
>
> A. Einstein.

1. Introduction

Einstein's general relativity theory of gravitation is remarkable and has been approved in various experiments, but some unreasonable physics has been assimilated on the way. For example:

(a) Given the rationality of electromagnetism and quantum theory, the concept of gravity being due to geometrical spacetime curvature is strangely detached and lacks physical mechanism or real substance, but it appears like an ethereal fabric of spacetime which propagates at the velocity of electromagnetism.

(b) Gravitational singularities can occur even though physicists understand that singularities are not founded on reality.

(c) Energy conservation is not well defined in general relativity theory. Thus, the ultimate source of kinetic energy acquired by a falling body is a problem.

(d) Inertial acceleration of a person inside a lift/elevator appears superficially like gravity but in detail it is energetically different from spacetime curvature.

(e) Fantastic non-falsifiable geometric theories for unification have been fabricated.

Given the experimental success of Einstein's theory, it is appropriate to search for a new solution of the field equations wherein gravitons exist analogous to the virtual-photon field of the electric force. Gravity is probably a quantum process because a gamma ray may decay to produce a proton and anti-proton with their gravitational and electromagnetic fields. The spacetime manifold has zero energy density in contrast to a graviton field and this difference influences the precession of Mercury's orbit enough to rule out the option of spacetime curvature.

In the following Sections the results from previous articles will be presented together to illustrate the prospects of Einstein's Equations. In Section 2 the electromagnetic nature of gravity will be supported through a new solution of the equations. Section 3 confirms the need for this solution by re-considering Mercury's orbital precession. Section 4 covers gravitational collapse to form dense bodies without singularities. Section 5 describes a model of the accelerating universe starting from a primeval electromagnetic particle. Section 6 shows how the new solution format can be applied to real models of the electron, proton, and charmonium, without point particles. Section 7 covers the hydrogen atom energy levels. Section 8 describes an auxiliary gravitational field which induces flat rotation curves and spiral structures in galaxies. Finally, in Section 9 the measured weight-reduction of a spinning wheel appears to be incompatible with theory of spacetime curvature.

2. The universal solution of Einstein's equations.

A few features of this solution will be quoted from reference [1] to demonstrate its quantum nature for gravity and correspondence with electromagnetism. Einstein searched for a covariant form of Poisson's equation and invented the concept of spacetime curvature to account for gravity acting through empty space. However, there is an alternative interpretation of gravity as a quantum field interaction, in Minkowski spacetime. Then the metric tensor component $g_{\mu\nu}$ describes the variance in the physical structure of a test particle due to interactions with a gravitational field.

Einstein's equations are written

$$-kT_{\mu\nu} = R_{\mu\nu} - (1/2)\, g_{\mu\nu}\, R\,, \tag{2.1}$$

where for the *new* solution, $R_{\mu\nu}$ represents a field tensor consisting of potential derivatives and is equated to the real energy and stress terms of $T_{\mu\nu}$. By solving Eq.(2.1) for the exterior spherically symmetric static field, while assigning $T_{\mu\nu}$ to the *real gravitational field energy and momentum*, we get

$$g_{44} = -g^{11} = (1 - GM/c^2 r)^2, \tag{2.2a}$$

with

$$T_4^4 = T_1^1 = -T_2^2 = -T_3^3 = +GM^2/8\pi r^4, \tag{2.2b}$$

which is independent of Schwarzschild's solution ($g_{44} = 1 - 2GM/c^2 r$). Gravitational force is then due to momentum transfer between the real graviton fields of bodies, existing in flat spacetime. The form of the $T_{\mu\nu}$ is analogous to the electromagnetic field and also indicates that field gravitons are circularly polarised and travel at the velocity of light.

In reference [1, Section 7] it is shown that the trajectory of a test graviton in a gravitational field is bent to convey momentum towards the gravitating body, thereby causing attraction in a classically understood manner.

Einstein's equations could theoretically provide a positive sign in Eq.(2.2a) signifying repulsive anti-gravity of a test particle in the gravitational field of a negative mass M. Therefore to avoid concepts of negative mass we will consider the electromagnetic analogy as follows. From reference [1, Section 13], the analogous expression to Eq.(2.2a) for *like* electron charges with ($\gamma^2 = g_{44}$) is

$$\gamma = (1 + e^2/m_o c^2 r)\,, \tag{2.5}$$

then a positive electric charge q_1 would repel a positive charge q_2 with force

$$F_{es} = (q_1/r^2)\, q_2\,. \tag{2.6}$$

However, in [1, Eq.(58)], the radial magnetic force between *like* current elements is found to be attractive

$$F_{em} = -(I_1 d\ell_1/r^2)(I_2 d\ell_2)\,. \tag{2.7}$$

This can be taken to mean that it is a magnetic aspect of electromagnetic gravitons that produces the attractive gravitational force.

In reference [1, Section 15] a graviton is proposed to have spin 2:

$$s_g = 2(h'/2\pi) = 2\hbar' \ , \tag{2.8}$$

where h' is a gravito-Planck's constant described in reference [6a] for planetary parameters in the Solar System which are functions of the atomic fine structure constant [6b]. This implies that there exists an equivalent *gravitational* dimensionless constant:

$$\frac{Gm^2}{\hbar' c} = \frac{1}{137} \quad \text{, where} \quad \frac{h'}{h} = \frac{Gm^2}{e^2}, \tag{2.9}$$

and (e/m) is the electronic charge/mass ratio.

3. The obscure precession of Mercury's orbit.

The orbit of planet Mercury has been calculated by several investigators [3] in order to explain the observed precession of the perihelion as the sum of general precession in longitude, perturbation by the planets, solar oblateness, and 43arcsec/cy for general relativity. However, when applying Eq.(2.2a) to the problem of Mercury's orbit, Weinberg [2, Eq.(8.6.10)] shows that the precession should be given by

$$\Delta\varphi = 5\pi GM/a(1-e^2) \approx 35.9 \text{arcsec/cy}. \tag{3.1}$$

To account for this 7arcsec/cy difference, an additional contribution to Mercury's orbital precession has recently been identified due to the Sun's motion around the barycentre [4]. This produces a quadrupole moment in the energy of Mercury which has to be included when integrating the equations of motion. Thus, imagine the Sun and Jupiter rapidly orbiting the barycentre so that the Sun takes on a blurred toroidal appearance. Mercury would then orbit the *average* position of the Sun at the barycentre, like for an oblate Sun, but there would be a quadrupole moment in its energy which would cause *precession*. Consequently, even for the Sun moving at 12.5m/s around the barycentre due to Jupiter, a small quadrupole component will remain which is calculated to generate 7arcsec/cy precession of Mercury's orbit. In effect, Mercury has to chase the Sun moving around the barycentre due to Jupiter, which makes Mercury's binding energy non-Newtonian. [By analogy, a pendulum will not swing sinusoidally while the suspension pivot is being moved around].

Hence to fit the observations, only 35.9arcsec/cy precession due to general relativity theory is required as in (3.1), rather than 43arcsec/cy for standard theory.

My error in original paper [1, Section 6] led to derived precession of 43arcsec/cy. To correct this error, (D/B) of Eq.(22b) therein should have been evaluated to produce

$$\frac{m_r}{\left(1-v^2/c^2\right)^{1/2}}\, r v_C = \frac{m_o}{\left(1-v^2/c^2\right)^{1/2}}\, r v_L \times \gamma^2 . \qquad (3.2)$$

On the left hand side is the coordinate angular momentum for a particle of coordinate mass m_r (representing Mercury, say) travelling at orbital velocity v_C . On the right, the first term is the local angular momentum for a particle of local mass m_o travelling at local velocity v_L . The final term ($\gamma^2 = g_{44}$) derives from ($m_r = \gamma m_o$) and ($v_C = \gamma v_L$). In addition to this angular momentum factor (γ^2) which causes precession there is a further precession term to be added due to special relativistic length contraction around the orbit. Namely, when the orbiting particle travels locally measured distance $2\pi r$, it actually travels coordinate distance $2\pi r\,(1- v^2/c^2)^{-1/2}$ which is interpreted as precession by the coordinate observer. For a circular orbit we have $(1- v^2/c^2)^{1/2} = \gamma^{1/2}$, consequently, to satisfy total particle covariance of action (angular momentum x angle) the particle actually travels $2\pi\gamma^{-5/2}$ coordinate radians per local revolution. Given this, the analysis *method* shown in reference [1, Eq.(23)] leads to the correct precession 35.9arcsec/cy. Thus, Nature rules consistently over all.

4. Gravitational collapse without singularities

Gravitational collapse of diffuse material has been investigated using the new solution of Einstein's equations of general relativity [5]. Accreting mass converts to kinetic energy then radiation, so that a singularity cannot be produced. Fully collapsed bodies now have real physical properties such as nuclear hard core density in collapsed stars, or around 10^4kg/*l* in the Galaxy centre, see Figure 1.

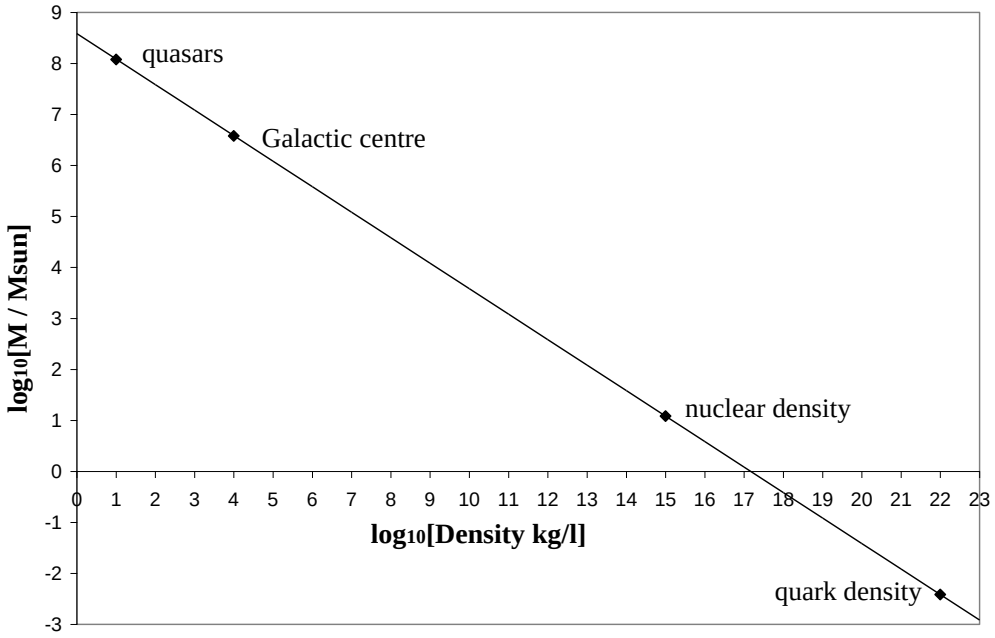

Fig. 1 Variation of body mass (in units of Solar mass) with density, for bodies at their gravitational radius.

In [1] it was shown that the gravitational field induces mass particles to fall by converting their own mass (potential energy) into kinetic energy which is lost as radiation upon impact. We can calculate how much free diffuse matter is required to build a body of current mass M up to its ultimate gravitational radius ($R_0 = GM_0/c^2$). For a mass element (δm) of free diffuse material falling inward, only a part (δM) is added to M:

$$\delta M = \delta m(1 - GM/c^2 r) \quad , \qquad (4.1)$$

This expression may be integrated for (δm) to find that it is impossible to build a body up to its gravitational radius because infalling matter is increasingly less effective at adding mass. Energetic γ-rays may be produced by single conversion of infalling particles. Collapse will cease when the core material pressure and kinetic energy are able to resist self-gravity. Any sudden collapse to a denser state may release enough energy to blast away the outer material in a super-nova event, leaving the imploded core to become a cool dark body. Thus, the original proposition of singularities should have driven a search for a natural solution to satisfy Eddington.

5. Model of the accelerating universe

Repulsive gravity at large distances can be introduced into the universal solution of Einstein's equations by adding a cosmological constant Λ, to exclude dark energy. For a new cosmological model [7], the big-bang singularity can be replaced by a granular primeval particle, and expansion rate is limited at the velocity of light. Then the inflation postulate, flatness and horizon problems in the standard model of cosmology do not arise. Graviton field properties can be related to proton dimensions via the electromagnetic factor (e^2/Gm^2).

5.1 Problems with the standard model

In reference [7], when using the standard Robertson-Walker metric:

$$ds^2 = -R^2(t)\left\{\frac{dr^2}{1-kr^2} + r^2 d\theta^2 + r^2 \sin^2\theta d\varphi^2\right\} + dt^2 \quad , \qquad (5.1)$$

the universe has non-Einsteinian super-luminal expansion at the beginning and also at large radii where Λ dominates, see Figure 2. In addition, the ethereal nature of space-time exploded into existence at the big-bang singularity followed by inexplicable inflation. Infinite space and the correct density of material were instantaneously created for the observed flat universe. Total energy, mass and size are not definitive. There are energy conservation, flatness and horizon problems. Continuous creation of dark energy throughout infinite space is now required. Evidently, after years of tackling these unsolved problems, a simpler intelligible model is to be welcomed.

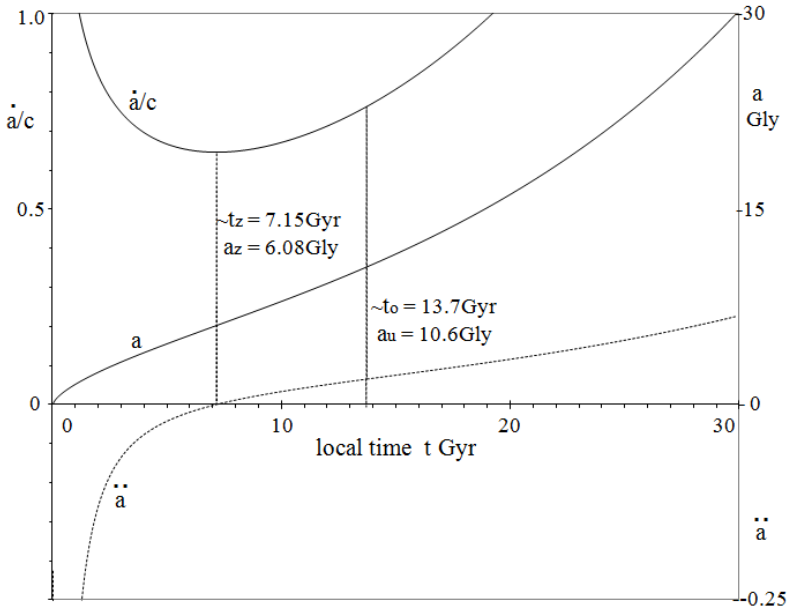

Fig.2. Friedmann-Lemaitre model: variation of expansion velocity relative to the velocity of light $(\dot{a}/c)$, radius (a, Gly), and acceleration ($\ddot{a}$) with universal time (t, Gyr). Universal mass has been set at $M_U = (4/3)\pi\rho a^3 = 1.085\text{x}10^{52}$ kg, with the change from deceleration to accelerated expansion occurring at radius 6.08Gly corresponding to epoch 7.15Gyr from the big-bang. The present age of the universe is 13.7Gyr and its radius is 10.6Gly.

5.2 External coordinate-observer cosmology: the ECO-model

We shall now consider the universal expansion from the point of view of an observer located at rest far outside of the material universe in field-free Minkowski spacetime where time-rate is not dilated by the expansion velocity [7]. Then to satisfy Einstein's relativity principles, this model will be controlled by the velocity of light, and the cosmological principle will not apply because the big-bang is just an explosion of a primeval particle into an existing volume of space at some arbitrary origin. Before exploding, this particle of finite mass, radius R_α and complex structure was in equilibrium internally. The current material universe now occupies a spherical volume of uniform density which is still expanding into free space, see Figure 3.

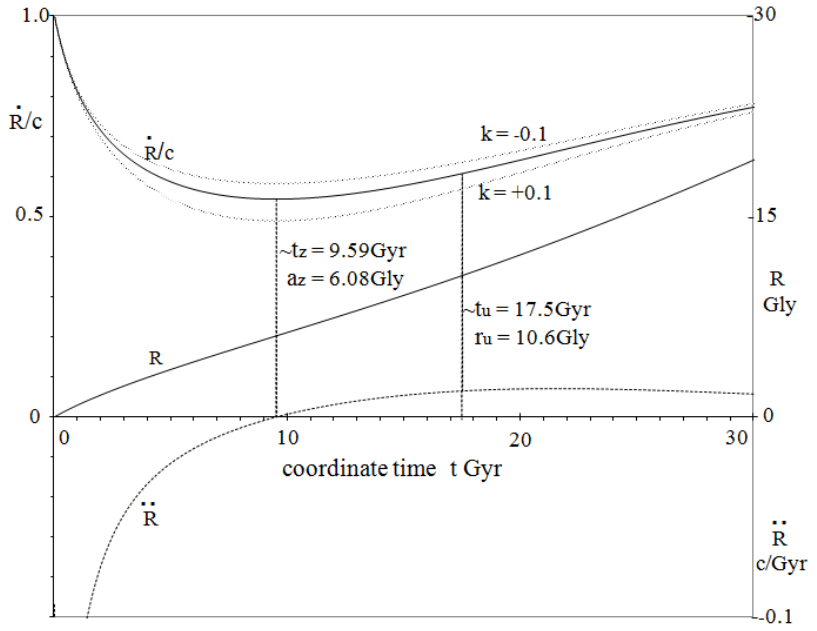

Fig. 3. New ECO-model, showing how the expansion velocity $(\dot{R}/c)$, the radius (R), and the acceleration $(\ddot{R})$ vary with *coordinate-frame time (t Gyr)*. Universal mass is currently (M_U = 1.085x10^{52} kg), with the change from deceleration to accelerated expansion occurring at radius 6.08Gly, corresponding to 9.59Gyr from the big-bang. The present coordinate age of the universe is 17.5Gyr, and its radius is 10.6Gly. For illustration purposes, the effect of a finite *k* value (±0.1) is also shown.

The metric for the ECO-model is to be:

$$ds^2 = -\frac{R^2(t)}{(1+kr^2/4)^2}\left\{dr^2 + r^2 d\theta^2 + r^2 \sin^2\theta d\varphi^2\right\} + \left(1-\frac{v^2}{c^2}\right)c^2 dt^2 \ . \qquad (5.2)$$

R(t) takes real units of radial length from *r* and represents the outer radius of the material universe, i.e. $R_\alpha < R(t) < \infty$, and $\dot{R}(t) = v \le c$. The primeval particle dimension R_α will be defined shortly. Coordinate-frame time *t* is that measured by an external observer situated at rest far from the expanding universal material. Local time (τ) for a co-moving observer is dilated due to the velocity of expansion as $[d\tau = dt(1-v^2/c^2)^{1/2}]$.

The primeval particle had all its material in thermodynamic equilibrium, circulating coherently at velocity *c*, before exploding and converting to mass plus much radiation which would have been mostly lost from the slower expanding mass.

Expansion is moderated by the velocity of light, allowing time for equalisation of the radiation temperature.

5.3 Properties of the primeval particle

The size of R_α can be specified if the primeval particle was of mass ($M_{\alpha u} \approx 7.75 \times 10^{52}$ kg) to produce a gravitational strength factor expressed as:

$$\frac{GM_{\alpha u} m_\ell}{\hbar c} = \left(\frac{e^2}{\hbar c}\right) \times \left(\frac{e^2}{Gm^2}\right) = \frac{1}{137}\left(\frac{E}{G}\right) \quad , \tag{5.3}$$

where ($m_\ell = m_p/9$) is the proton-pearl/gluon mass in [8], $\hbar$ is Planck's constant/2π, ($e^2/\hbar c \approx 1/137$) is the fine structure constant, ($e/m = E^{1/2}$) is the electronic charge/mass ratio, and ($E/G = 4.1659 \times 10^{42}$). The primeval mass relative to a proton-pearl mass is then:

$$\frac{M_{\alpha u}}{m_\ell} = \left(\frac{m}{m_\ell}\right)^2 \left(\frac{E}{G}\right)^2 = 4.169 \times 10^{80} \ . \tag{5.4}$$

This primeval mass $M_{\alpha u}$ exploded into the pre-existing infinite space to yield free radiation plus the residual universal mass ($M_U = 1.085 \times 10^{52}$kg).

A proton-pearl classical *electromagnetic* radius is given by:

$$r_{o\ell} = e^2/m_\ell c^2 = 1.38 \times 10^{-17} \text{ m} \ , \tag{5.5}$$

whereas a *gravitational* radius for mass $M_{\alpha u}$ may be:

$$R_{\alpha u} = GM_{\alpha u}/c^2 = 6.08\text{Gly} = r_{o\ell}(E/G) \ , \tag{5.6}$$

therefore the primeval mass $M_{\alpha u}$ was like a *super-pearl* of radius ($R_\alpha = r_{o\ell}$). Such a particle is unlike Lemaitre's 'primeval atom' in which space and time were created during disintegration.

According to our proton model [8], the super-pearl consisted of many smaller spinning seeds which may have grown into strings of galaxies with dense cores. These therefore did not have to form entirely from subsequently accreted matter. Some of the primeval material might have been restricted in its expansion by bordering pressure so as to become dark matter, but if it now falls into stars it may well convert into radiation.

6. Models of particles

Einstein's equations are proposed to be universal and applicable to particles as for a unified field theory. They can describe electromagnetic, nuclear, strong and weak force fields by introducing experimental data. The particles themselves must be structured, rather than the theoretical singularities which are convenient for describing interactions *between* particles.

6.1 Model of the Electron

The electron model [9] is based on the universal solution of Einstein's equations of general relativity [1] applied to electromagnetism. The electron body has the design of a helically wound hollow torus, see Figure 4. Total mass of the electron constitutes this core plus the exterior radial field energy. Such a structured electron experiences relativistic time dilation, length contraction, and energy variation due to velocity or applied force fields.

Charge is due to a radial field of electromagnetic quanta tied to their core source but propagating out and back at the velocity of light. For opposite charges, the field is inductive and causes attractive motion but no energy exchange occurs. Then for example, a positron and electron at rest far apart may attract each other and fall together by converting their own rest mass energy to kinetic energy. Upon collision, two photons are emitted of total energy $2h\nu = m_{o(+)}\,c^2 + m_{o(-)}\,c^2$. During the fall at separation *r*, where the coordinate *rest* mass would be [$m_r = m_o(1-e^2/m_oc^2r)$], we have (in cgs units for simplicity):

$$2\left(\frac{e^2}{r}\right) \;=\; 2\left(m_oc^2 - m_rc^2\right) \;=\; 2\left\{\frac{m_rc^2}{\left(1-v^2/c^2\right)^{1/2}} - m_rc^2\right\}. \qquad (6.1.1)$$

[coordinate PE lost] [coordinate rest mass lost] [coordinate KE gained]

Evidently, potential energy is the same thing as rest mass energy and may convert to kinetic energy of the particle.

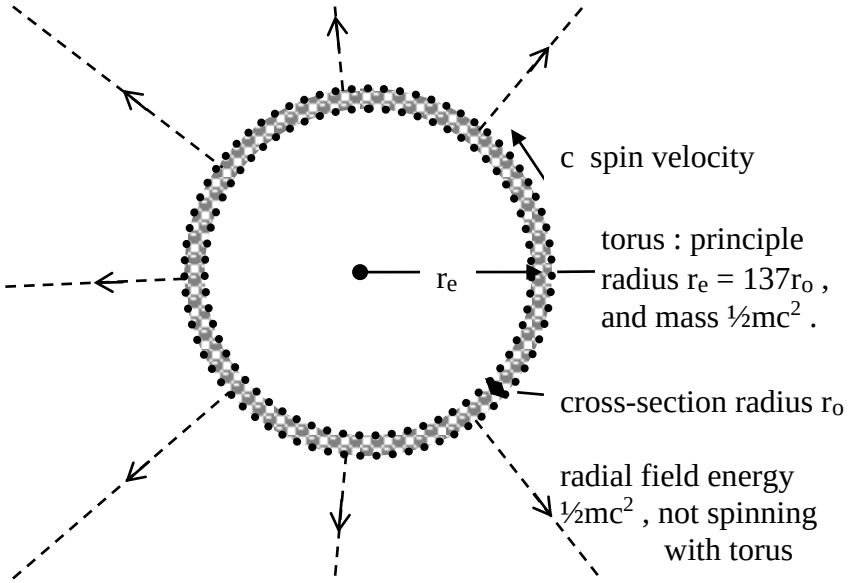

Fig.4 Schematic diagram of toroidal electron model.

For charges of the same sign to approach each other, it is necessary to increase their kinetic energy (initial velocity v_1) by means of a separate accelerator field. Then in a head-on collision, this KE converts to rest mass energy as the particles slow towards zero velocity due to the repulsive field. At the instant of closest approach (R) we have:

$$2\,m_o c^2 + 2\left(\frac{e^2}{R}\right) = \frac{2m_o c^2}{\left(1 - v_1^{\,2}/c^2\right)^{1/2}} = 2m_1 c^2 \quad , \qquad (6.1.2)$$

where the left side is total rest mass energy, and on the right side is the relativistic initial rest mass plus kinetic energy. Again, potential energy (e^2/R) represents rest mass energy with R decreasing as v_1 increases. In addition, the electron radius also decreases as its kinetic energy increases, ($r_{o1} = e^2/m_1c^2$). Furthermore, the electron charge increases to cause running of the fine structure constant, see [10]. This all leads to the electron acting more point-like.

For the metric tensor component $[\gamma^2 = (1 - e^2/mc^2r)^2]$, Einstein's field equations for the electric field of a spherically-symmetric static electron may be written:

$$8\pi(E/c^4)T_1^1 = 8\pi(E/c^4)T_4^4 = \frac{1}{r^2}\frac{d}{dr}\left[r(1-\gamma^2)\right], \qquad (6.1.3)$$

$$-8\pi(E/c^4)T_2^2 = -8\pi(E/c^4)T_3^3 = \frac{\gamma}{r^2}\frac{d}{dr}\left(r^2\frac{d\gamma}{dr}\right)+\left(\frac{d\gamma}{dr}\right)^2, \qquad (6.1.4)$$

where $\sqrt{E}$ = (e/m) is the electronic charge/mass ratio. Upon substituting γ, these simplify to:

$$T_1^1 = T_4^4 = \frac{e^2}{8\pi\, r^4}\ , \text{and}\quad T_2^2 = T_3^3 = -\frac{e^2}{8\pi\, r^4}\ . \qquad (6.1.5)$$

Here, the negative sign for T_2^2 means that the electric field quanta have tangential momentum orthogonal to the radial direction. The radial momentum density T_1^1 is equal to the energy density T_4^4 because the field quanta travel at the velocity of light with unitary helicity. Total energy of the field may be found by integration from the classical electron radius $(r_o = e^2/mc^2)$ to infinity:

$$W_0 = \int_{r_o}^{\infty} 4\pi\, r^2 T_4^4 dr = \frac{e^2}{2r_o} = \frac{1}{2}mc^2\ . \qquad (6.1.6)$$

This explains why renormalisation in QED theory, using the classical electron radius (r_0), is a way of handling a real electron.

6.2 Model of the Proton

Our proton model [8] is compatible with electron and muon models, and the hadronic potential is *analogous* to the Yukawa potential. Einstein's equations of general relativity can be employed to predict a nucleonic coupling constant.

The Klein-Gordon wave equation will be taken as the basis of our inter-nucleon potential:

$$\frac{1}{c^2}\frac{\partial^2\psi}{\partial t^2} = \nabla^2\psi - \left(\frac{m_\ell c}{\hbar}\right)^2\psi = \nabla^2\psi - \left(\frac{1}{r_\ell}\right)^2\psi\ , \qquad (6.2.1)$$

where ($r_\ell = \hbar/m_\ell c$ = 1.89278 fm) is the proton-pearl Compton radius, rather than the standard pionic radius. If wavefunction Ψ is proportional to potential V(r), then:

$$V(r) = -a_Y\frac{\exp-(r/r_\ell)}{r}\ , \qquad (6.2.2)$$

where a_Y represents a hadronic/nuclear charge.

For a relativistic expression using Einstein's equations, we must define the metric tensor component for the proton of mass m_p:

$$\gamma^2 = \left\{1 - 2\left(\frac{a_Y{}^2}{m_p c^2}\right)\frac{\exp-(r/r_\ell)}{r}\right\} \quad . \tag{6.2.3}$$

Given ($\gamma = 0$) at the *effective* proton radius ($r_p = \hbar/m_p c = 0.2103$fm) this becomes:

$$\gamma^2 = \left\{1 - \left(\frac{r_p}{r}\right)\exp-\left(\frac{r - r_p}{r_\ell}\right)\right\}. \tag{6.2.4}$$

And, the empirical coordinate potential V_c is given by:

$$a_Y V_c = \left(m_p c^2\right)(\gamma - 1) \, . \tag{6.2.5}$$

Thus the hadronic charge strength a_Y in terms of the electronic charge *e* is given by:

$$a_Y{}^2 \approx \left(\frac{m_p c^2 r_p}{2}\right)\exp\left(\frac{r_p}{r_\ell}\right) \approx 76.570171\, e^2 \quad , \tag{6.2.6}$$

so a nucleonic coupling constant α_Y is definable as:

$$\alpha_Y = \frac{a_Y{}^2}{\hbar c} \approx 76.6\left(\frac{1}{137}\right) \approx \frac{5}{9} \approx \frac{1}{\sqrt{3}} \quad . \tag{6.2.7}$$

Using (6.2.3), energy-momentum tensor components for a conserved spherically-symmetric radial field evaluate to:

$$8\pi\left(\frac{Y}{c^4}\right)T_2^2 = [\frac{(a_Y{}^2/m_p c^2)}{r_\ell{}^2}]\times\left(\frac{1}{r}\right)\exp-\left(\frac{r}{r_\ell}\right) \quad . \tag{6.2.8}$$

$$8\pi\left(\frac{Y}{c^4}\right)T_4^4 = [\frac{(a_Y{}^2/m_p c^2)}{r_\ell}]\times\left(\frac{-2}{r^2}\right)\exp-\left(\frac{r}{r_\ell}\right) \quad . \tag{6.2.9}$$

see (6.1.3), (6.1.4) and [1]; Y is the NN hadronic constant equal to ($137e^2/m_p{}^2$). Integration of T_4^4 from r_p to infinity yields the total field energy equal to half the proton mass energy:

$$W = \int_{r_p}^{\infty} T_4^4 \, 4\pi \, r^2 dr = -\tfrac{1}{2} m_p c^2 \quad . \tag{6.2.10}$$

Hard core repulsion will be attributed to field modulation due to the spinning proton core. Gluonic charge ($g \approx 11.94e$) operating around the spin-loop is also involved. This effect can be incorporated by changing (6.2.4) thus:

$$\gamma_{NQ}{}^2 = \left\{1-\left[1-\left(\frac{m_p}{m_\ell}\frac{g}{a_Y}\right)\left(\frac{a_Y{}^2}{m_p c^2 r}\right)\exp-\left(\frac{r-r_p}{r_p}\right)\right]\times\left(\frac{r_p}{r}\right)\exp-\left(\frac{r-r_p}{r_\ell}\right)\right\}. \quad (6.2.11)$$

and the nucleon natural quiescent potential is then given by:

$$a_Y V_{NQ} = \left(m_p c^2\right)\left(\gamma_{NQ}-1\right) \ . \quad (6.2.12)$$

Now for pp interactions, the expression (6.2.11) has to be adjusted to take into account the finite size of a *colliding* proton such that the closest approach distance is actually $2r_p$ in contrast to the above r_p for the infinitesimal theoretical test particle. Therefore, (6.2.11) becomes a *coupling* metric tensor component:

$$\gamma_{COUPLING}{}^2 = \left\{1-\left[1-\frac{9g\alpha_Y}{a_Y}\left(\frac{r_p}{r-r_p}\right)\exp-\left(\frac{r-2r_p}{r_p}\right)\right]\times\left(\frac{r_p}{r-r_p}\right)\exp-\left(\frac{r-2r_p}{r_\ell}\right)\right\}. \quad (6.2.13)$$

The *coupling* potential is given by:

$$a_Y V_{COUPLING} = \left(m_p c^2\right)\left(\gamma_{COUPLING}-1\right) \ . \quad (6.2.14)$$

Given this, a good fit to experimental data can be achieved by squaring and scaling to derive the real nucleon *interaction* potential:

$$\begin{aligned} a_Y V_{INTERACTION} &= (a_Y V_{COUPLING})^2 \times (2\pi/\alpha_Y)/(m_p c^2) \\ &= (2\pi r_p)\times(V_{COUPLING})^2 \end{aligned} \ . \quad (6.2.15)$$

This is plotted in Figure 5, and it fits the $^1S_0$ component given by Stoks et al. (1994) after adding relativistic correction, see [8].

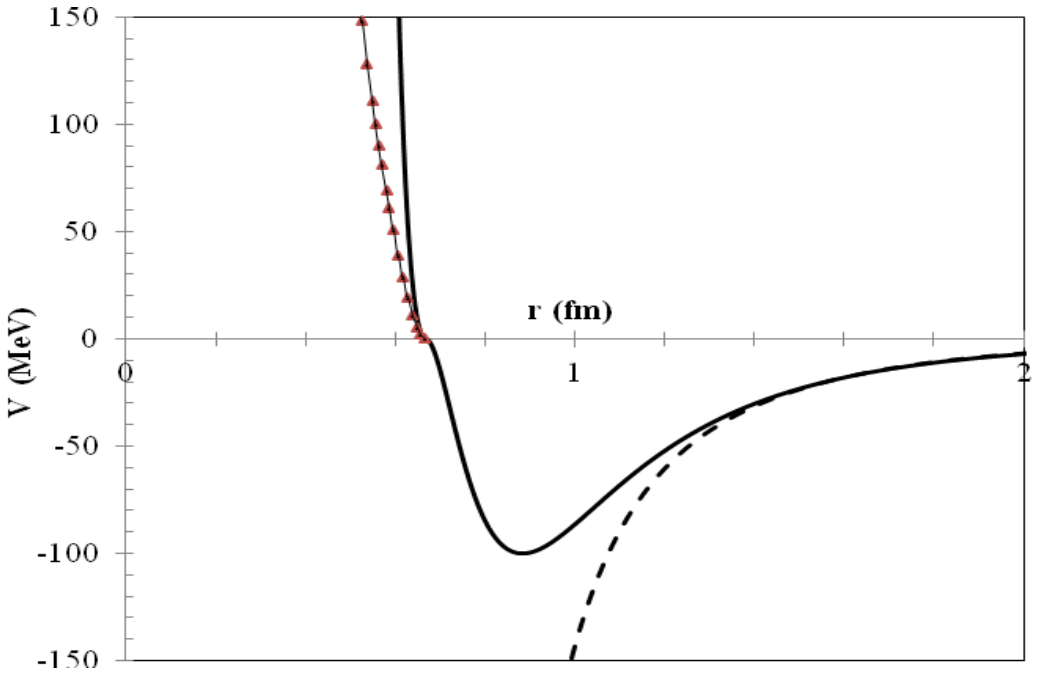

Fig.5. Nucleon interaction potential. Bold-line: potential Eq.(6.2.15). Triangles: relativistic correction. Dashed-line: enhanced attraction between a nucleon and anti-nucleon.

In our proton model [8], we identify the gluons of QCD theory as the 9 pearls constituting 3 trineons (analogous to quarks) carrying colour charge quanta. The logarithmic potential is taken to describe the gluon colour field between trineons:

$$V(r) = \frac{m_p c^2}{2} \ln\left(\frac{r}{r_p}\right) \quad , \tag{6.2.16}$$

where the proton radius is [$r_p = 137(e^2/m_p c^2)$]. Potential (6.2.16) will apply to a linear field, such as for a flux-tube of gluons with colour charge linking the trineons around the proton spin-loop. The metric tensor component for Einstein's equations will take the form:

$$\gamma = \left[1 + \frac{V(r)}{m_p c^2}\right] = \left[1 + \frac{1}{2}\ln\left(\frac{r}{r_p}\right)\right] \quad , \tag{6.2.17}$$

then the tangential momentum/stress density for the colour field charge particles, is derived as:

$$8\pi\left(\frac{S}{c^4}\right)T_2^2 = \left|\frac{\gamma}{2r^2}\right| - \left|\frac{1}{2r}\right|^2 \quad . \tag{6.2.18}$$

The longitudinal momentum density T_1^1 is made compatible with T_2^2 by specifying the form:

$$8\pi\left(\frac{S}{c^4}\right)T_1^1 = 8\pi\left(\frac{S}{c^4}\right)T_4^4 \Rightarrow \left|\frac{-1}{2r}\right|^2 + \left|\frac{1}{2r}\right|^2 \quad . \tag{6.2.19}$$

Integration of this T_4^4 from ($r = r_{ot} = Sm_p/c^2$) to ($r = \infty$), will yield the total colour field energy amounting to 25% of the proton mass energy:

$$W = -\int_{r_{ot}}^{\infty} T_4^4 (4\pi {r_{ot}}^2) dr = \tfrac{1}{4} m_p c^2 \quad . \tag{6.2.20}$$

This colour field material is wrapped around the proton spin-loop multiple times.

Our proton model has been used to help interpret the running of (α_S) with momentum transfer in a collision process, see [10]. The strong coupling constant derived therein (α_S = 1.0406845) describes the gluon coupling which binds the proton's components together. It can be related to the above nuclear constant (α_Y = 0.55876) of (6.2.7) which binds nuclei together:

$$\alpha_S = \frac{g^2}{\hbar c} \approx \left(\frac{e_n}{2}\right)^2 \alpha_Y \approx \left(\frac{e_n}{2}\right)^2 \frac{{a_Y}^2}{\hbar c}, \quad \text{or} \quad g \approx \left(\frac{e_n}{2}\right) a_Y . \tag{6.2.21}$$

where ($g \approx 11.94e$) is an equivalent gluonic charge and (e_n = 2.718282). The *total* charge carried by gluons is ($a_T = a_Y + g$) so there is a strength constant (α_T) given by:

$$\alpha_T = (a_Y + g)^2 / \hbar c \approx 3\alpha_S \ , \tag{6.2.22}$$

which reminds us of 3 trineons in a proton. Then (6.2.16) can also be written:

$$V(r) \approx \frac{g^2}{(2\pi r_p / 3)} \ln\left(\frac{r}{r_p}\right) \ , \tag{6.2.23}$$

where the denominator equals the distance between trineons around the spin-loop.

6.3 A Model of Charmonium

A composite model of charmonium has been developed, based on the logarithmic confinement potential [11]. The quark-antiquark pair of total mass M_C orbit around the centre of mass with their colour fields confined within a toroidal flux-tube of characteristic radius r_{q1}, see Figure 6. Then the potential energy for the

antiquark in the field of the quark may be written as:

$$V(r_1) = \frac{M_C c^2}{2\sqrt{2}} \ln\left(\frac{r_1}{r_{q1}}\right), \tag{6.3.1}$$

which implies the metric tensor component:

$$\gamma = \left\{1 + \frac{1}{2\sqrt{2}} \ln\left(\frac{r_1}{r_{q1}}\right)\right\} \quad . \tag{6.3.2}$$

There is a solution of Einstein's Equations for a static linear colour field found in a flux-tube. Upon introducing γ from (6.3.2) we get:

$$8\pi\left(\frac{S}{c^4}\right)T_2^2 = \left(\frac{\gamma}{2\sqrt{2}\ r_1^{\,2}}\right) - \left(\frac{1}{2\sqrt{2}\ r_1}\right)^2 \quad . \tag{6.3.3}$$

$$8\pi\left(\frac{S}{c^4}\right)T_1^1 = 8\pi\left(\frac{S}{c^4}\right)T_4^4 \Rightarrow \left|\frac{-1}{8\ r_1^{\,2}}\right| + \left|\frac{1}{8r_1^{\,2}}\right| \quad . \tag{6.3.4}$$

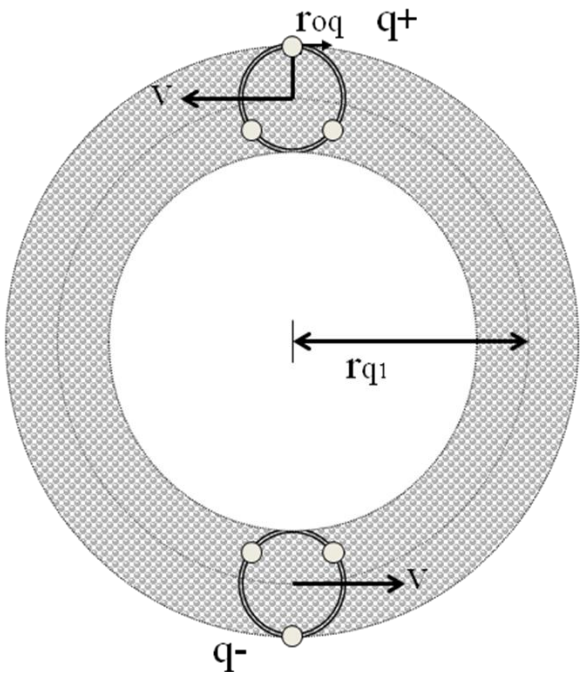

Fig. 6 Schematic diagram of charmonium in which quark and antiquark gluons emit their colour fields into a toroidal flux-tube.

Integration of energy density T_4^4 from ($r_z = r_{q1}\exp(-2\sqrt{2})$, $\gamma = 0$) to ($r_1 = \infty$) will then lead to the total colour field energy. This integration represents the colour field wrapped in many turns around the circumference:

$$\left(\frac{S}{c^4}\right)\int_{r_z}^{\infty} T_4^4 (4\pi\, r_z{}^2)dr \Rightarrow \left|\frac{-r_z}{16}\right| + \left|\frac{r_z}{16}\right| \quad . \tag{6.3.5}$$

On the left, $(4\pi r_z^2)$ is a workable representative area for the flux-tube. Upon setting [$r_z = SM_C/c^2$], then the total *colour* field energy is 12.5% of the charmonium total mass energy:

$$W = -\int_{r_z}^{\infty} T_4^4 (4\pi\, r_z{}^2)dr = \frac{1}{8} M_C c^2 \quad . \tag{6.3.6}$$

The source gluons carrying the colour field account for the same amount of mass energy. Tangential momentum density may also be integrated to get a similar result:

$$\left(\frac{S}{c^4}\right)\int_{r_z}^{\infty} T_2^2 (4\pi\, r_z{}^2)dr = \left|\frac{-r_z}{16}\right| + \left|\frac{r_z}{16}\right| \quad , \tag{6.3.7}$$

therefore on average the colour field charge and quanta have unitary helicity.

All these results for the proton spin-loop and toroidal charmonium structure point to the realistic nature of the *logarithmic* potential. On the other hand, it appears that the popular Coulomb + linear potential [$V(r) = -\kappa/r + r/a^2$] *cannot* be viable because the corresponding momentum density T_2^2 would integrate to infinity, as would the *classical* energy density term $(dV(r)/dr)^2$.

7 General relativistic theory of hydrogen energy-levels

Einstein's equations of general relativity may be applied to the hydrogen atom if electromagnetic field energies of the proton and electron are introduced, [1] [12]. This solution produces hydrogen energy-levels identical to the Dirac solution [13] when spin is neglected. The concept of space-time curvature has to be replaced by a description of a particle's time and length variation caused by the field environment; which is analogous to Lorentz transformation for particles in an acceleration field.

Briefly, an electron of *local* rest mass m_o at radius *r* from the proton would have a coordinate rest mass [$m_r = (m_o - e^2/c_o^2 r) = \gamma\, m_o$] due to loss of potential energy (mass energy). If the electron is actually orbiting at *local* velocity v_{local}, its relativistic local mass is increased to {$m_l = m_o /[1 - (v_{local}/c_o)^2]^{1/2}$}. Then the *coordinate* total electron energy should be ($E = \gamma\, m_l\, c_o^2$), which will be confirmed from the geodesic equations as follows.

The geodesic equations for the electron trajectory in the proton's Coulomb field will be taken as [14] (Tolman 1934, p207):

$$\gamma^2 (dt/ds)^2 - \gamma^{-2} (dr/ds)^2 - r^2 (d\phi/ds)^2 = A \ , \qquad (7.1)$$

$$\gamma^2 (dt/ds) = B \ , \qquad (7.2)$$

$$r^2 (d\phi/ds) = D \ , \qquad (7.3)$$

where ds is an element of local time or space, [$\gamma^2 = (1 - e^2/m_o c_o^2\, r)^2$] is to be the metric tensor component, (A = 1) for particles, (A = 0) for quanta, B represents total electron energy, D is an angular momentum constant.

From Eq.(7.1) and Eq.(7.2) for a *circular* electron orbit we have:

$$\gamma^2 - r^2 (d\phi/dt)^2 = \gamma^4 / B^2 \quad , \qquad (7.4)$$

where [$r(d\phi/dt) = v_{coord}$] is the electron velocity according to the coordinate observer. And from Eq.(7.1), putting (A = 0, ds = 0), we get for the coordinate velocity of light in the orbit, ($c_{coord} = \gamma\, c_o$). Therefore, all velocities in the orbit are reduced by factor γ, according to the coordinate observer. Equation (7.4) may then be written:

$$\gamma^2 / B^2 = 1 - (v_{coord}/\gamma c_o)^2 = 1 - (v_{coord}/c_{coord})^2 = 1 - (v_{local}/c_o)^2 . \qquad (7.5)$$

We need to simplify this by relating γ to (v/c) through two conditions: (a) For large radius orbit we expect [$e^2/2r \approx (1/2) m_o v^2$]. (b) For minimum radius at the electron classical radius ($r = r_o$), we have ($v_{local} = c_o$), where ($\gamma = 0$) and ($e^2/r_o = m_o\, c_o^2$). In general therefore, ($e^2/r = m_o v^2_{local}$), and then {$\gamma = [1 - (v_{local}/c_o)^2]$}. Thus, from Eq.(7.5) the electron total energy constant may take different forms:

$$B = \gamma / [1 - (v/c)^2]^{1/2} = [1 - e^2/m_o c_o^2\, r]^{1/2} = [1 - (v/c)^2]^{1/2} = \gamma^{1/2} . \qquad (7.6)$$

So the orbiting electron has coordinate energy $E = Bm_oc_o^2 = \gamma\, m_l\, c_o^2$ as derived earlier. Equation (7.2) shows that the orbiting electron's local time element ds is decreased relative to coordinate time dt by $\gamma[1-(v/c)^2]^{1/2}$, due to local field plus its own velocity.

When ($r = n^2a_o$), ($a_o = \hbar^2/m_oe^2$), ($\alpha = e^2/\hbar c$) for hydrogen, this gives coordinate electron energy:

$$B = (E/m_oc_o^{\,2}) = (1-\alpha^2/n^2)^{1/2},$$
$$\text{then} \quad E = m_oc_o^{\,2}(1-\alpha^2/n^2)^{1/2}, \tag{7.7}$$

which is identical to Dirac's particular solution for radial quantum number equal to zero. This result is very important because it demonstrates successful application of Einstein's general relativity field theory of particles to quantum theory. That is, the Coulomb field and gravitational field are similar conserved tensor fields obeying Einstein's equations. Einstein's interpretation of his *geometric* theory cannot lead to Eq.(7.7). For stability there are exactly *n* de Broglie wavelengths around the circular orbit due to the electron's *increased local* relativistic mass, in spite of its *reduced coordinate* energy. However, the question arises as to how the general relativity analysis which produced Eq.(7.7) can satisfy the Dirac analysis built upon special relativity. It appears that Dirac's analysis is automatically set so that the wavefunctions satisfy *local* dimensions of scale and time (the special relativity frame) in order to fit the *real local* de Broglie wavelengths.

8 Auxiliary gravitational field in galaxies.

A theory has been developed of a relativistic auxiliary gravitational field [15] which accounts for the empirical success of Milgrom's modified Newtonian dynamics theory. Essential links with atomic physics rule out any applicability of spacetime curvature. This so-called *gravito-cordic field* theory explains the observed structure within galaxies in addition to reducing the need for dark matter. Field resonance causes galactic material to form into flat rotation curves. The angular momentum proportional to mass-squared relationship is also attributed to this field, and gravitational lensing is significant.

8.1 Gravito-cordic field theory.

A characteristic acceleration factor a_o is fundamental to this field and has been optimised in a way to include atomic physics:

$$a_o = 1.116x10^{-10}\,ms^{-2} \quad . \tag{8.1}$$

The gravito-cordic field exists within a galaxy *in addition* to normal Newtonian gravity (g_N), and orbiting bodies experience both forces simultaneously acting towards the galactic centre. The total gravitational acceleration has been derived as:

$$g_\omega = g_N + a_o \left\{ \frac{(g_N/a_o)^{1/2}}{[(g_N/a_o)+1]} \right\} \quad . \tag{8.2}$$

This field satisfies the solar system criteria and the flat galaxy rotation curves already fitted with Milgrom's MOND calculations. Figure 7 shows how the asymptotic relationship holds for g_ω, so only small changes are required in the mass distribution predicted by Milgrom's g_μ.

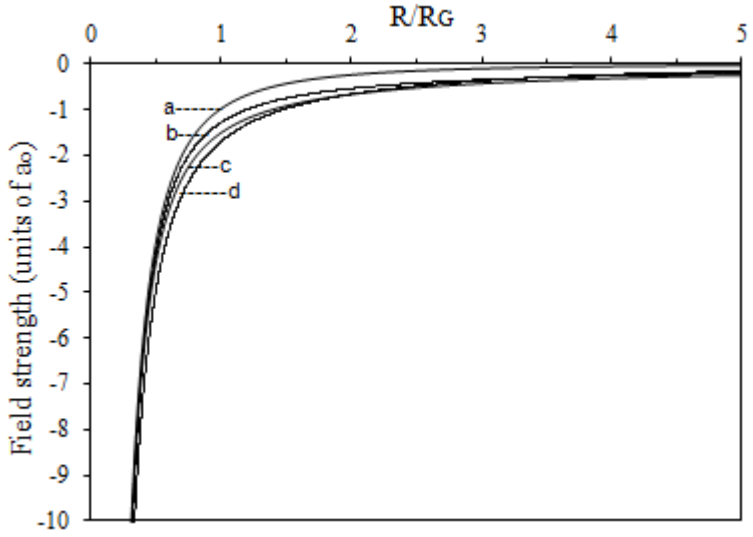

Fig. 7. Comparison of accelerations versus normalised radius
(a) g_N Newton, (b) g_μ Milgrom, (c) g_ω Wayte, and (d) g_M Moffat,.

Einstein's equations are a mathematical description of *any* conserved energetic field so they can be applied to a conserved gravito-cordic field. For example, consider a galaxy in which surface mass density is exponential with radius, and then the galactic mass distribution is given by integration:

$$M = \int_o^r 2\pi r \rho_s dr = M_{max}\left[1-\left(1+\frac{r}{r_c}\right)\exp\left(-\frac{r}{r_c}\right)\right], \tag{8.3}$$

where M_{max} is the total disk mass and r_c is the characteristic radius. Now, let this radial mass distribution be roughly equivalent to a spherical galaxy of bulk density:

$$\rho_b = \frac{M_{max}}{4\pi r_c^{\,2}}\left(\frac{\exp - r/r_c}{r}\right), \tag{8.4}$$

so that Einstein's equations describing the spherically-symmetric static field in polar coordinates can be applied, (see [14] p242). For the line element:

$$ds^2 = -e^{\lambda}dr^2 - r^2 d\theta^2 - r^2\sin^2\theta d\varphi^2 + e^{\nu}dt^2, \tag{8.5}$$

the tensor component T_4^4 is expressed in terms of $e^{-\lambda}$ thus:

$$8\pi\left(\frac{G}{c^4}\right)T_4^4 = -\frac{1}{r^2}\frac{d}{dr}\left\{r\left(e^{-\lambda}-1\right)\right\}. \tag{8.6}$$

Now for an interior field suspended by angular momentum, $e^{-\lambda}$ is a potential function and the field strength can be equated to the total field in (8.2):

$$\left(\frac{c^2}{2}\right)\frac{d}{dr}\left(e^{-\lambda}-1\right) = a_o\left\{\frac{g_N}{a_o} + \frac{(g_N/a_o)^{1/2}}{\left[(g_N/a_o)+1\right]}\right\}. \tag{8.7}$$

Upon introducing mass (8.3), it is necessary to integrate this numerically to get $e^{-\lambda}$. For large galaxies ($M_{max} = 10^{11}M_{\Theta}$, $r_c \sim 7$kpc), such that on average ($GM_{max}/r_c^2 a_o \sim 2.5$), then for ($R = r/r_c$) we have:

$$\frac{g_N}{a_o} = \left(\frac{GM}{a_o r^2}\right) = \left(\frac{GM_{max}}{a_o r_c^{\,2}}\right)\left(\frac{1}{R^2}\right)\left[1-(1+R)\exp(-R)\right]. \tag{8.8}$$

Upon introducing this into (8.7), integration yields:

$$e^{-\lambda} \approx 1-\left(\frac{2GM_{max}}{c^2 r_c R}\right)\left[4.5\left(1+\frac{R}{8.5}\right)\left(1-\exp(-R/1.5)\right)\right], \tag{8.9}$$

so that the negative potential energy at small R is 3 times the Newtonian value alone.

If the gravito-cordic term is removed from the right side of (8.7), then only the Newtonian field is considered such that integration for $e^{-\lambda}$ has the form:

$$e^{-\lambda} = 1-\left(\frac{2GM_{max}}{c^2 r_c R}\right)\left[(1-\exp(-R)\right], \tag{8.10}$$

then we can evaluate tensor component T_4^4 in equation (8.6) as:

$$T_4^4 = \left(\frac{M_{max} c^2}{4\pi r_c} \right) \left(\frac{\exp(-r / r_c)}{r^2} \right), \qquad (8.11)$$

which is an equivalent energy density not bulk density (8.4) because galactic orbital angular momentum has not been incorporated.

By comparison, the total field (8.9) substituted in (8.6), yields for small *r* :

$$T_4^4 \approx \left(\frac{M_{max} c^2}{4\pi r_c} \right) \left(\frac{4.5 \exp(-r / 1.5 r_c)}{r^2} \right), \qquad (8.12)$$

which is a stronger *effective* energy density due to the gravito-cordic field.

8.2 Gravitational lensing.

Observations indicate that the gravito-cordic field causes relativistic light deflection analogous to normal gravity. Figure 8 illustrates the calculated deflection for a cluster of 100 galaxies (10^{13} M_Θ) within radius 1Mpc.

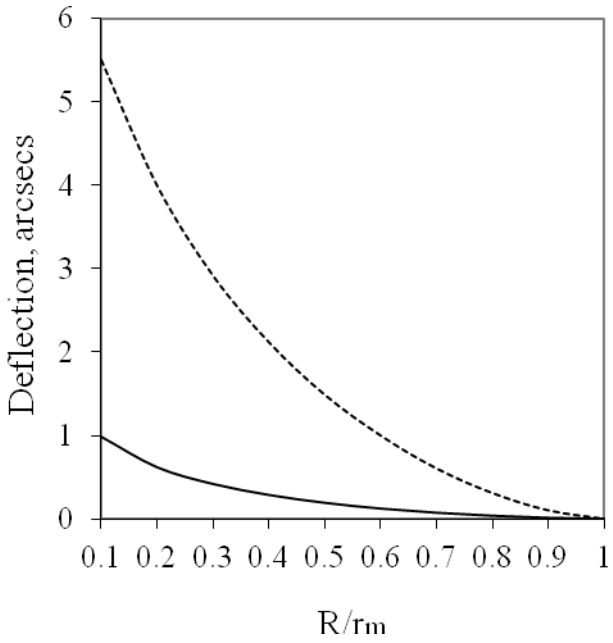

Fig. 8 The relativistic deflection of light travelling through a cluster of galaxies due to the Newtonian component (——), and the gravito-cordic component (- - - -). Cluster size has been set at: r_m = 1Mpc, and Q = M/r = $10^{13} M_\Theta$ / Mpc.

8.3 Resonance and quantisation in galaxy orbits.

It is thought that the gravito-cordic field induces resonance in disc galaxy orbits to produce flat rotation curves, bar or spiral structures and galactic rings. Hydrogen atoms are the main source of the field because their *gravitational de Broglie wavelength* shows a fit to galactic dimensions. Matter will accumulate in the grand spiral and other energy node-lines to produce inter-arm branches.

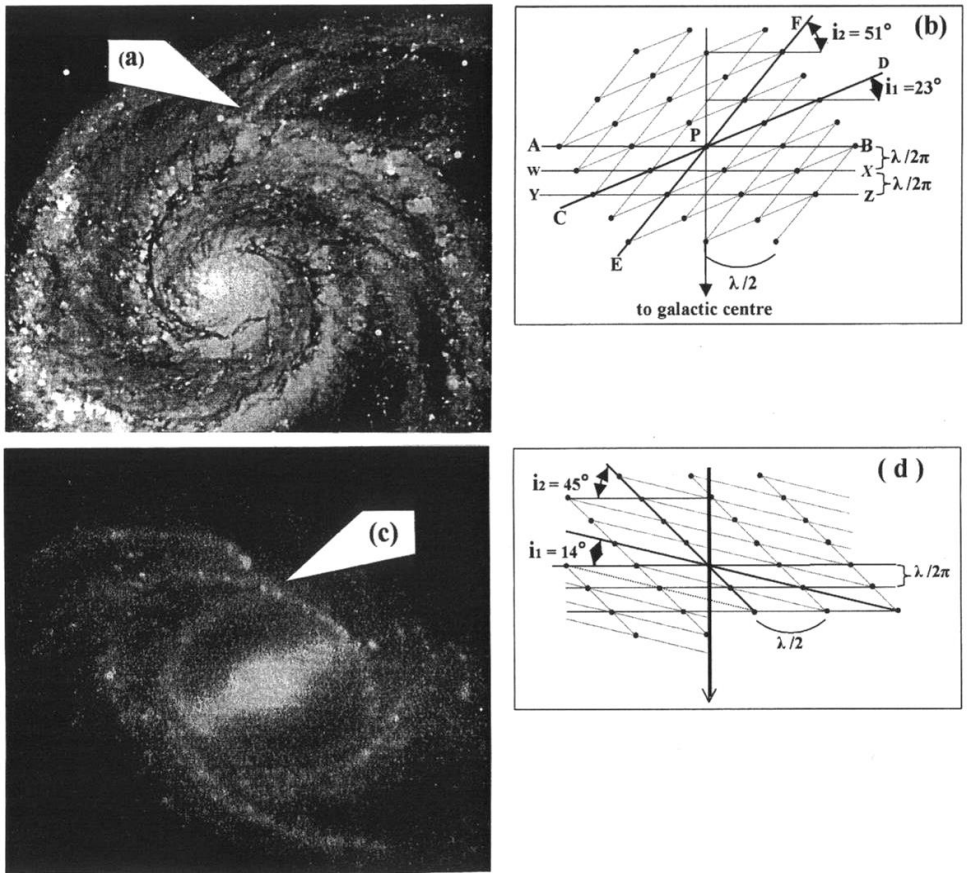

Fig. 9. The proposed quantisation node pattern for two galactic spiral arm/branch intersection regions, marked in the photographs. The galactic material in both the main spiral and branch is seen to be aligned along the node lines. Parts a, b, M51; parts c, d, NGC2523.

Figure 9(a) illustrates M51 with one such branch marked for analysis. The arm/branch intersection region is magnified in (b) to reveal the proposed myriad of quantisation nodes. Thus, the main spiral arm at P lies at 23deg from circular and has tangent CPD which joins nodes of the same phase. At the same time, the branch

tangent EPF lies at 51deg from circular and also joins nodes of similar phase. The figure shows that angles i_2 and i_1 are simply connected by:

$$\cot(i_2) = \cot(i_1) - \pi/2 \quad . \tag{8.13a}$$

The barred galaxy NGC2523 has an inner ring and a strongly bifurcated spiral arm, see Figure 9 (c). After correction for inclination of the galaxy, part (d) shows the proposed nodal pattern at the fork where the spiral arm lies at 14deg from circular and the branch lies at 45deg, so that:

$$\cot(i_2) = \cot(i_1) - \pi \quad . \tag{8.13b}$$

8.4 The J proportional to M^2 law.

According to gravito-cordic theory, there is an optimum material velocity for implementing the quantisation phenomenon in primeval hydrogen:

$$v_z = (4\pi/137^2)c \approx 201 \text{ kms}^{-1}. \tag{8.14}$$

Then, within the universal expansion, turbulent spherical volumes may have separated when they had this preferred rotation velocity:

$$v_z \approx [G\rho(4/3)\pi]^{1/2} r_z \quad , \tag{8.15}$$

where ρ is the average gas density and $M = (4/3)\pi\rho r_z^3$. Variation in ρ produced a range of galactic masses. After separation, the angular momentum of a randomly rotating spherical volume is

$$J \approx (3/5) M v_z r_z \ , \text{ or } \quad J \approx pM^2 \ . \tag{8.16}$$

Here p is a constant equal to $(3/5)(G/v_z)$, as drawn on Figure 10, namely:

$$p_{201} = 2.00 \text{ x}10^{-15} \text{ g}^{-1} \text{ cm}^2 \text{ s}^{-1} = 2.00 \text{ x}10^{-16} \text{ kg}^{-1} \text{ m}^2 \text{ s}^{-1} . \tag{8.17}$$

Clusters of galaxies and disc galaxies agree with (8.17) while other systems correspond to their own *preferred* quantisation wavelengths, see [16]. Classically, there is no explanation for the specific sizes of existing bodies nor for the gaps between them.

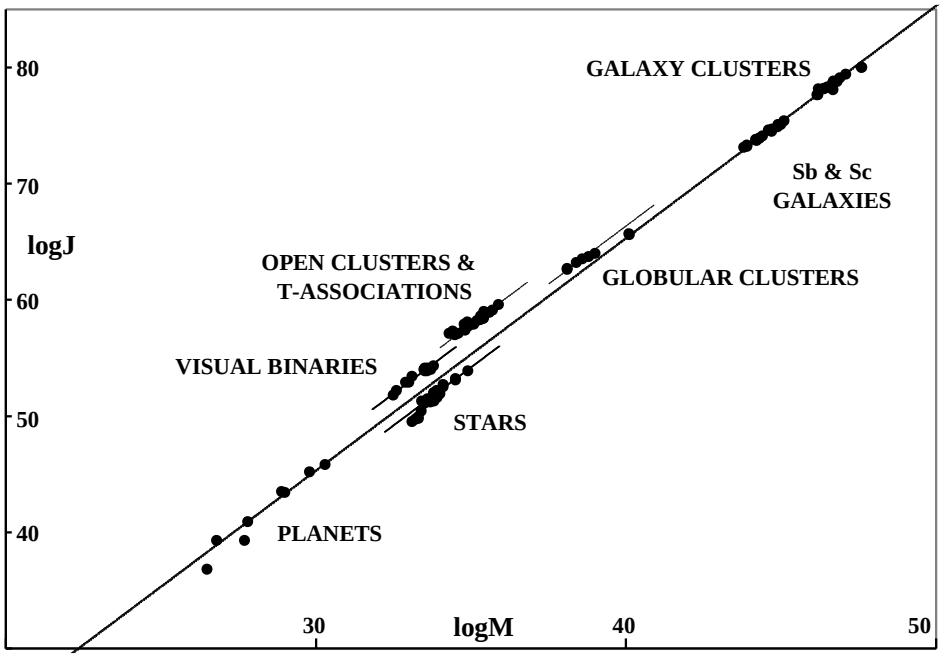

Fig. 10 The angular momentum versus mass^2 relationship for astronomical bodies, showing a theoretical straight line for $J = 2.00 \times 10^{-15} M^2$ over 40 decades.

9 The phenomenon of weight-reduction of a spinning wheel.

An investigation has been conducted into weight-reduction of a spinning wheel [17]. When subjected to forced precession and controlled lifting, a spinning wheel does indeed lose 8% of its weight, as measured by a load-cell. That is, some of the gravitational potential energy acquired during lifting is supplied by the horizontal force causing the precession. Consequently, the vertical lifting force is less than Mg on average, see Figure 11. The explanation for this weight-reduction follows directly from the requirement of energy conservation throughout the process. No thrust or mass-reduction occurs. Analysis for this effect was enabled by using the Principle of Equivalence.

It is comprehensible that Earth's real graviton field possessing energy and transverse momentum (2.2b) may interact with the spinning wheel to convert horizontally applied work into vertical potential energy. On the other hand, it could be a problem for energy-free vacuum spacetime geometry to do this.

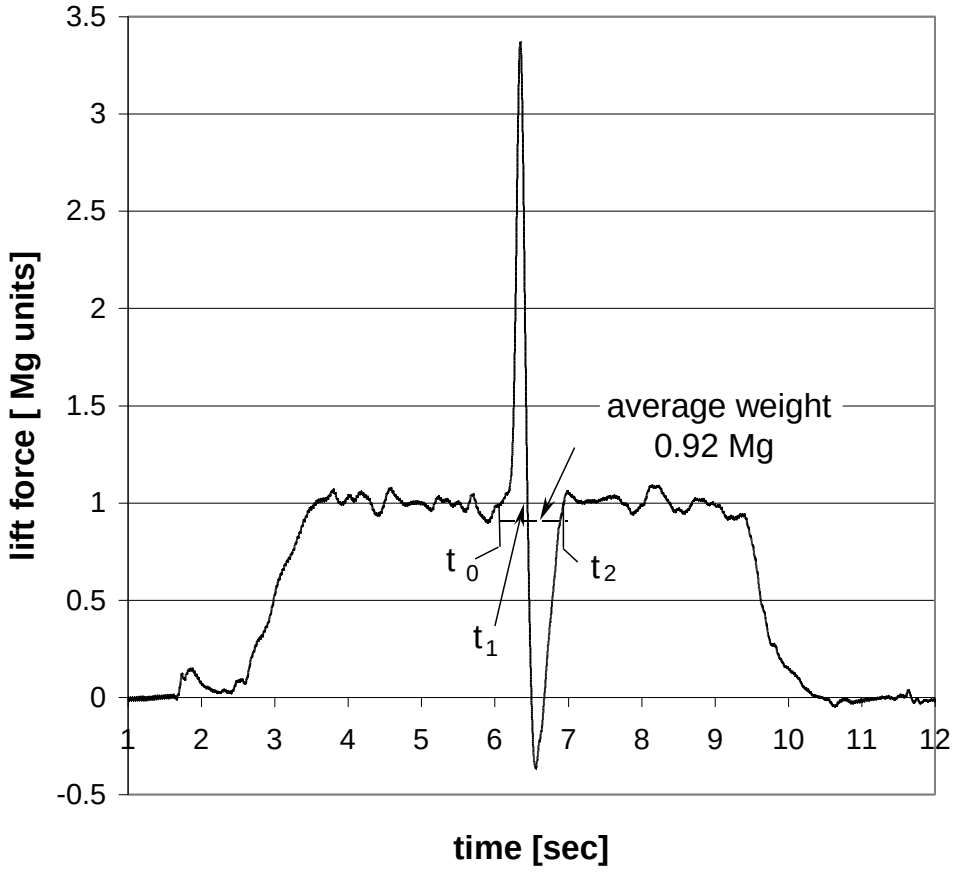

Fig. 11 A typical measure of gyroscope weight during the lifting and forced precession period. Normal precession from 3.5 to 6 seconds gives weight Mg as expected. Lifting and pulling first increases the measured weight considerably as the wheel is accelerated upwards. Then as the lifting and pulling are decreased, the wheel rises upward for a while due to its inertia and its measured weight falls well below Mg and even negative as kinetic energy converts to gravitational potential energy. This excursion below Mg is greater in area than that above and may be regarded as evidence for weight-reduction overall.

Conclusion

The electromagnetic nature of gravity was suggested through a new solution of Einstein's equations of general relativity. Need for this solution was confirmed by considering Mercury's orbital precession in detail. Gravitational collapse to form a singularity was then proven to be impossible. A model of the accelerating universe starting from a primeval electromagnetic particle was described which did not suffer from the many standard model problems. The new solution was applied to other forces of nature to show that particles have unique structures consisting of electromagnetic material. Real models of the electron, proton, and charmonium, led

to derivation of the strong coupling constant. Each particle has mass due to core material plus field energy. Hydrogen atomic energy levels were calculated to be compatible with Dirac's analysis. A gravito-cordic field operating in galaxies was described which encourages the formation of flat rotation curves, spiral structures, and the angular momentum proportional to mass^2 law. Finally, the observed weight-reduction of a spinning wheel was described but it appeared to be incompatible with spacetime curvature theory. Given these new applications for Einstein's Equations, useful knowledge will increase.

References

[1] Wayte, R., The universal solution of Einstein's equations of general relativity. Astrophys Space Sci. (1983) **91**:345. http://adsabs.harvard.edu/abstract_service.html

[2] Weinberg, S., Gravitation and Cosmology: Principles and Applications of the General Theory of Relativity. (1972) John Wiley & Sons, Inc.

[3a] Brouwer, D., & Clemence, G.M., Methods of Celestial Mechanics. (1961) Academic Press, New York

[3b] Clemence, G.M., Rev. Mod. Phys. (1947) 19, 361-4

[4] Wayte, R., The obscure precession of Mercury's perihelion (Revised3). (15 Feb 2016) http://viXra.org/abs/1201.0064

[5] Wayte, R., On gravitational collapse (Revised). (2019) http://viXra.org/abs/1910.0410

[6a] Wayte, R., Quantisation in stable gravitational systems. The Moon and the Planets. (1982) **26**, 11-32

[6b] Wayte, R., Evidence for Quantisation in Planetary Ring Systems. (2010) http://vixra.org/abs/1002.0017

[7] Wayte, R., On the accelerating universal expansion (Revised). (2019) http://viXra.org/abs/1904.0199

[8] Wayte R., A model of the proton (Rev). (2019) http://viXra.org/abs/1910.0329

[9] Wayte, R., A model of the electron. (2010) http://viXra.org/abs/1007.0055

[10] Wayte, R., Running of electromagnetic and strong coupling constants (Rev2). (2017) http://viXra.org/abs/1704.0095

[11] Wayte R., A model of charmonium (Revised). (2019) http://viXra.org/abs/1910.0356

[12] Wayte R., Theory of an electro-cordic field operating in quantum systems I (Rev). (2019) http://vixra.org/abs/1911.0077

[13] Dirac P A M., The Principles of Quantum Mechanics. (1962) Clarendon Press, Oxford

[14] Tolman R C., Relativity, Thermodynamics and Cosmology, reprint. (2011) Dover, NY

[15] Wayte, R., An auxiliary gravitational field operating in galaxies (Revised). (2019) http://viXra.org/abs/1910.0486

[16] Wayte, R., Quantisation of the auxiliary gravitational field in astronomical systems. (2011) http://viXra.org/abs/1101.0040

[17] Wayte, R., The phenomenon of weight-reduction of a spinning wheel. (2007) Meccanica 42:359-364. https://www.researchgate.net/publication/227146624_The_phenomenon_of_weight-reduction_of_a_spinning_wheel